Title

Dopamine D2 receptor signaling in the brain modulates circadian liver metabolomic profiles

Journal

Proceedings of the National Academy of Sciences of the United States of America, 119(11)

ISSN

0027-8424

Authors

Cervantes, Marlene
Lewis, Robert G
Della-Fazia, Maria Agnese
et al.

Publication Date

2022-03-15

DOI

10.1073/pnas.2117113119

PNAS RESEARCH ARTICLE | PHYSIOLOGY OPEN ACCESS

Dopamine D2 receptor signaling in the brain modulates circadian liver metabolomic profiles

Marlene Cervantes[a,b,1], Robert G. Lewis[a,c,1], Maria Agnese Della-Fazia[d], Emiliana Borrelli[a,c,2], and Paolo Sassone-Corsi[a,b]

Edited by Joseph Takahashi, The University of Texas Southwestern Medical Center, Dallas, TX; received September 16, 2021; accepted February 8, 2022

The circadian clock is tightly intertwined with metabolism and relies heavily on multifaceted interactions between organ systems to maintain proper timing. Genetic and/or environmental causes can disrupt communication between organs and alter rhythmic activities. Substance use leads to altered dopamine signaling followed by reprogramming of circadian gene expression and metabolism in the reward system. However, whether altered dopamine signaling in the brain affects circadian metabolism in peripheral organs has not been fully explored. We show that dopamine D2 receptors (D2R) in striatal medium spiny neurons (MSNs) play a key role in regulating diurnal liver metabolic activities. In addition, drugs that increase dopamine levels, such as cocaine, disrupt circadian metabolic profiles in the liver, which is exacerbated by loss of D2R signaling in MSNs. These results uncover a strict communication between neurons/brain areas and liver metabolism as well as the association between substance use and systemic deficits.

circadian metabolism | reward | striatum | circadian rhythm | addiction

Significance

We analyzed the liver metabolome of mice deficient in the expression of the dopamine D2 receptor (D2R) in striatal medium spiny neurons (iMSN-D2RKO) and found profound changes in the liver circadian metabolome compared to control mice. Additionally, we show activation of dopaminergic circuits by acute cocaine administration in iMSN-D2RKO mice reprograms the circadian liver metabolome in response to cocaine. D2R signaling in MSNs is key for striatal output and essential for regulating the first response to the cellular and rewarding effects of cocaine. Our results suggest changes in dopamine signaling in specific striatal neurons evoke major changes in liver physiology. Dysregulation of liver metabolism could contribute to an altered allostatic state and therefore be involved in continued use of drugs.

Substance use disorders affect millions of people worldwide (1). The rewarding properties of substances, such as alcohol, nicotine, opioids, and psychostimulants, are linked to their ability to increase dopamine levels in brain areas that control emotions and induce pleasure (2). Drug intake modifies neuronal plasticity and is at the start of the process of addiction, which leads vulnerable individuals to continually seek and abuse these substances despite the adverse consequences on their lives. Addiction causes long-term molecular and cellular changes in brain circuits involved in signaling reward (3).

The striatum is a key reward region that receives dopaminergic inputs from the ventral tegmental area and substantia nigra. Dorsal and ventral regions of the striatum are critical for the effects of addictive drugs. The dorsal striatum is critical for the motor-stimulating effects of drugs, decision-making, and habitual behavior (4–6). However, the ventral striatum (particularly the nucleus accumbens [NAcc]) is involved in reward evaluation and incentive-based learning (7–9). Prominent cell types in the striatum are the inhibitory γ-aminobutyric acid–producing medium spiny neurons (MSNs), which make up 90 to 95% of the striatal neuronal population (10). Two output pathways originate from MSNs: the direct pathway formed by MSNs (dMSNs) expressing dopamine D1 receptors (D1R) and the indirect pathway formed by MSNs (iMSNs) expressing dopamine D2 receptors (D2R). Dopamine signaling in dMSNs and iMSNs is critical for the integration of and response to rewarding stimuli. Dysregulation of activity in these neurons has been extensively implicated in addiction (11).

The development and progression of substance use disorders generates perturbations in circadian rhythms (12, 13). Disrupted circadian rhythms may result from a combination of substance abuse and genetic and environmental factors (12, 13), which interfere with metabolism. Transcription factors CLOCK and BMAL1 regulate the rhythmic expression of mammalian clock–controlled genes (14). Among these genes, *Period* (*Per1-3*) and *Cryptochrome* (*Cry1-2*) subsequently inhibit CLOCK–BMAL1-mediated gene expression (15), driving a transcriptional–translational circadian feedback loop that operates in a 24-h cycle.

Importantly, the circadian clock is a network of biological pacemakers found in virtually all tissues of the body. These pacemakers direct and maintain proper rhythmic homeostasis through various endocrine and metabolic pathways (16, 17). Circadian clocks are influenced by environmental cues such as food intake, physical exercise, and social activities that show tissue-specific effects (18, 19). Indeed, the same clock genes display tissue-specific profiles dictated by the transcriptional machinery unique to each tissue and condition; thus, generating large networks of oscillating clocks.

Interorgan communication is critical for maintaining organismal synchrony and systemic homeostasis, as demonstrated by the plastic response of metabolites among various organs following an environmental stressor (20). We investigated the interorgan

Author affiliations: [a]INSERM U1233, Center for Epigenetics and Metabolism, University of California, Irvine, CA 92697; [b]Department of Biological Chemistry, University of California, Irvine, CA 92697; [c]Department of Microbiology and Molecular Genetics, University of California, Irvine, CA 92697; and [d]Department of Medicine and Surgery, University of Perugia, Perugia 06132, Italy

Author contributions: E.B. and P.S.-C. designed research; M.C., R.G.L., and M.A.D.-F. performed research; M.C. and R.G.L. analyzed data; and M.C., R.G.L., and E.B. wrote the paper.

The authors declare no competing interest.

This article is a PNAS Direct Submission.

[1]M.C. and R.G.L. contributed equally to this work.

[2]To whom correspondence may be addressed. Email: borrelli@uci.edu.

This article contains supporting information online at http://www.pnas.org/lookup/suppl/doi:10.1073/pnas.2117113119/-/DCSupplemental.

Published March 10, 2022.

communication between the striatum and the liver by analyzing wild-type (WT) mice and their littermates carrying a cell-specific deletion of D2R in iMSNs (iMSN-D2RKO). We further deepened our studies by analyzing this interorgan communication in response to a widely abused drug, cocaine, as an external stressor. This way, we assessed whether cocaine-induced dopamine elevation in the striatum might affect liver homeostasis and the circadian fluctuation of metabolites. Interestingly, in addition to metabolic changes found in untreated mice between genotypes, cocaine administration in iMSN-D2RKO mice leads to reprogramming of circadian gene expression in the NAcc (21). While an acute cocaine challenge induces variation in the profiles of rhythmic metabolites in the liver of WT mice, in iMSN-D2RKO mice, loss of D2R in the striatum alters this rhythmic profile. We determined the time-dependent distribution of metabolites in the liver after acute cocaine treatment. Furthermore, we observed dynamic diurnal changes in the number and class of rhythmic metabolites in saline-treated mice. Strikingly, the livers of mice administered cocaine showed a dampened response to the time-of-day variances. In combination with loss of D2R in iMSNs, cocaine increased the total number of oscillating metabolites compared to WT mice. These results indicate that environmental and genetic changes in brain areas central for the rewarding effects of cocaine affect liver metabolic responses. Thus, we reveal a tight interorgan interaction in response to cocaine, which strongly modifies the basal physiology and circadian rhythms not only in the brain (22) but also in the liver. These results highlight an unexpected level of communication between striatal neurons and liver metabolism, which might also contribute to development of substance use disorders.

Results

Diurnal Metabolic Behavioral Phenotypes of iMSN-D2RKO Mice. In the striatum, dopamine receptor signaling is critical for the control of physiological responses, including eating (23) and motor behavior (24), which greatly influence metabolism. Thus, we analyzed the impact of typical or altered dopamine D2R signaling in the striatum on physiological parameters through comparisons between WT mice and littermates with the specific deletion of D2R in iMSNs (iMSN-D2RKO).

Since food intake and motor activity influence body weight (25), we recorded the weights of mice of both genotypes from birth to adulthood. Interestingly, we observed no differences in body weight during the first 5 wk after birth; thereafter, iMSN-D2RKO mice had reduced weight in comparison to WT controls [two-way ANOVA mixed-effects analysis; time $F_{(16,436)} = 548.7$, $P < 0.0001$; genotype $F_{(1,41)} = 78.08$, $P < 0.0001$; interaction $F_{(16,436)} = 2.24$, $P = 0.0040$] (Fig. 1*A*). Thus, we examined diurnal activity and energy expenditure along with eating and drinking behaviors in calorimetric cages, which could explain this difference between adult iMSN-D2RKO and WT mice. In agreement with previous data (26), we found that in actimetric cages, iMSN-D2RKO mice show significantly lower beam break counts than WT littermates during their active phase (dark phase, $P = 0.0099$) but not during their inactive phase (light phase, $P = 0.9922$) (Fig. 1*B*). Moreover, energy expenditure of iMSN-D2RKO mice was markedly reduced in both dark ($P = 0.0001$) and light phases ($P = 0.0125$) (Fig. 1*C*) compared to WT littermates. Relatedly, iMSN-D2RKO mice showed decreased chow consumption (Fig. 1*D*) compared to their WT littermates during the dark phase ($P = 0.0019$) but not the light phase ($P = 0.5951$); the same trend was observed for water intake (dark, $P = 0.0345$; light, $P = 0.4292$) (Fig. 1*E*). Interestingly, despite decreased chow consumption and lower weight, adult iMSN-D2RKO mice had significantly higher gonadal fat content than their WT counterparts ($P = 0.0001$) (Fig. 1*F*).

Profiling of the Circadian Metabolome in iMSN-D2RKO Mouse Liver. The liver plays a central role in metabolic processes. Both genetic and environmental challenges are capable of reprogramming the liver metabolome (21, 27–32) along the circadian cycle. Thus, we analyzed hepatic metabolites during the circadian cycle in iMSN-D2RKO and WT siblings. For this, we harvested liver tissue from mice of both genotypes every 4 h spanning a full circadian cycle for a total of six time points (Zeitgeber time [ZT] 3, 7, 11, 15, 19, and 23). Gene expression of core clock genes confirmed the rhythmicity of the samples used for metabolite analyses (*SI Appendix*, Fig. S1). The hepatic metabolome was quantified by mass spectrometry. Circadian rhythmicity was analyzed using JTK_CYCLE (33), a nonparametric test, to determine the number of significantly oscillating ($P < 0.05$; with a period of ∼24 h) circadian metabolites for each genotype (Fig. 2*A*). We found that nearly 20% of the 180 metabolites analyzed were significantly oscillating ($P < 0.05$) in both genotypes (34 and 32 metabolites in the WT and iMSN-D2RKO mice, respectively). This finding is in general agreement with the percentage of rhythmic metabolites identified in previous studies (21, 27–32). Importantly, ∼80% of the oscillating metabolites were lipids, including acylcarnitines, phosphatidylcholines, sphingomyelins, and lysophosphatidylcholines. The remaining oscillating metabolites belonged to the amino acids and biogenic amines groups (Fig. 2*B*). Specifically, ∼32% of the rhythmic metabolites in the WT and 46% in the iMSN-D2RKO livers were amino acid–derived metabolites. Phase analyses revealed ZT8 and ZT14 to ZT18 as the main time points at which circadian metabolites peak in abundance (Fig. 2*C*). Likewise, the amplitudes of the oscillating metabolites were nearly consistent in both WT and iMSN-D2RKO mice (*SI Appendix*, Fig. S2*A*). These data show that rhythmic metabolites in WT and iMSN-D2RKO livers display similar circadian patterns. However, in addition to a subset of metabolites that oscillate in both genotypes, and despite the similarities in circadian parameters, comparisons of individual metabolites oscillating in each genotype identified unique metabolites exclusively oscillating either in WT or in iMSN-D2RKO livers (Fig. 2 *D* and *E*). Surprisingly, in iMSN-D2RKO mice, ∼44% of liver metabolites lost rhythmicity compared to WT controls. In addition, ∼40% of metabolites show de novo oscillations in iMSN-D2RKO livers not observed in the WT. Among the metabolites analyzed, acylcarnitines show the greatest loss of rhythmicity in iMSN-D2RKO livers (Fig. 2 *F* and *G*). We analyzed the circadian gene expression profile of the metabolic enzyme carnitine palmitoyltransferase 1A (*Cpt1a*), which catalyzes the transfer of an acyl group onto carnitines in the production of acylcarnitines, which showed a significantly elevated expression in iMSN-D2RKO mouse liver at ZT11 and ZT15 by qPCR (*SI Appendix*, Fig. S2*B*). It is tempting to speculate that this increased expression is likely to contribute to the loss of rhythmicity of the five acylcarnitines in the iMSN-D2RKO livers (*SI Appendix*, Fig. S2*C*). Conversely, a threefold increase was found for newly oscillating metabolites in the iMSN-D2RKO livers, which consisted of some amino acids, including methionine and leucine. Metabolites consistently rhythmic in both genotypes included amino acids, biogenic amines, acylcarnitines, and phosphatidylcholines. These analyses demonstrate a previously ignored influence of

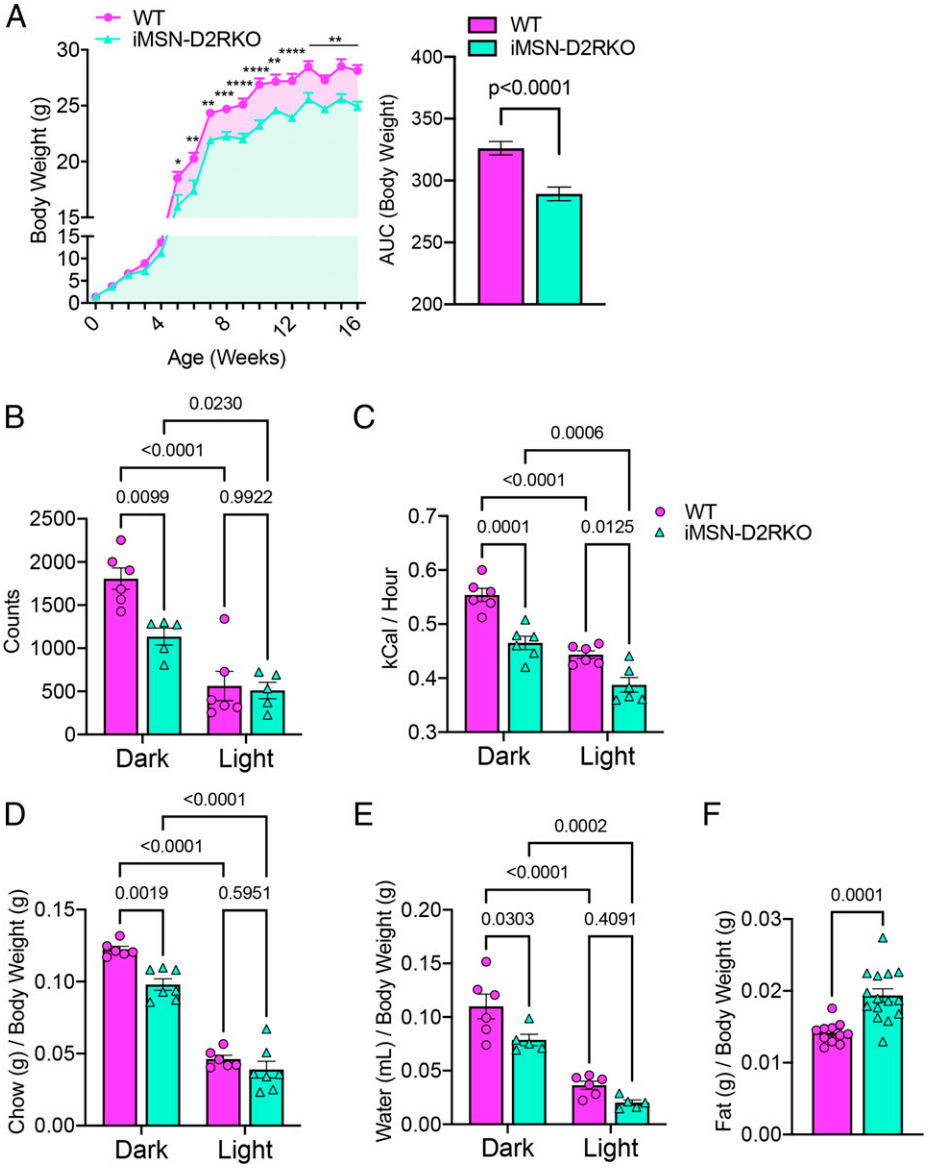

Fig. 1. Diurnal metabolic behavioral phenotypes of iMSN-D2RKO mice. (*A*, *Left*) Body weights of WT (pink circles) and iMSN-D2RKO (blue triangles) mice were recorded once a week from birth to 16 wk of age. A two-way ANOVA mixed-effects analysis was performed; time $F_{(16,436)} = 548.7$, $P < 0.0001$; genotype $F_{(1,41)} = 78.08$, $P < 0.0001$; interaction $F_{(16,436)} = 2.24$, $P = 0.0040$; Bonferroni post hoc test: $^{*}P < 0.05$, $^{**}P < 0.01$, $^{***}P < 0.001$, $^{****}P < 0.0001$. *Right*, Area under the curve (AUC) from the body weight curve (*left*); unpaired Student's *t* test, $P < 0.0001$. (*B*) Diurnal activity of iMSN-D2RKO and WT mice presented as beam break counts in an actimetric cage during the light and dark phases; two-way ANOVA; phase $F_{(1,18)} = 50.22$, $P < 0.0001$; genotype $F_{(1,18)} = 7.540$, $P = 0.0133$; interaction $F_{(1,18)} = 5.533$, $P = 0.0302$. (*C*) Energy expenditure while in the metabolic cages was recorded in iMSN-D2RKO and WT mice; two-way ANOVA; phase $F_{(1,22)} = 271.3$, $P < 0.0001$; genotype $F_{(1,22)} = 14.99$, $P = 0.0008$; interaction $F_{(1,22)} = 4.352$, $P = 0.0488$. (*D*) Bar graph showing chow consumption [phase $F_{(1,18)} = 84.35$, $P < 0.0001$; genotype $F_{(1,18)} = 10.88$, $P = 0.0040$; interaction $F_{(1,20)} = 1.995$, $P = 0.1731$]. (*E*) Water intake of iMSN-D2RKO and WT mice in the metabolic cages as a portion of their body weight; two-way ANOVA; phase $F_{(1,18)} = 84.35$, $P < 0.0001$; genotype $F_{(1,18)} = 10.88$, $P = 0.0040$; interaction $F_{(1,20)} = 1.995$, $P = 0.1731$. (*F*) Gonadal fat of iMSN-D2RKO mice and their WT controls was dissected and weighed after metabolic testing; Student's *t* test, $P = 0.0001$. All WT and iMSN-D2RKO mice were males; $n \geq 5$ as indicated by individual data points in each graph.

striatal neurons on the liver, as distinct metabolites show altered circadian profiles in the livers of iMSN-D2RKO mice compared to WT.

Loss of D2R in iMSNs Alters the Rhythmic Liver Metabolome of Cocaine-Treated Mice. The impact of absent D2R signaling in iMSNs on circadian liver metabolites under basal conditions (saline) prompted us to analyze the effect of a dopaminergic challenge on liver metabolism in WT and mutant mice. We used cocaine, which is known to increase dopamine levels in the striatum and disrupt the circadian cycle (22). For this, we compared the liver metabolome in saline- and cocaine-treated (administered at ZT3) WT and iMSN-D2RKO mice. Strikingly, ~73% of the metabolites oscillating in saline-treated WT mice lost their rhythmicity after cocaine administration. Only ~26% of the previously oscillating metabolites in saline conditions retained their rhythmicity after acute cocaine treatment (Fig. 3 *A* and *B*). The amplitude of circadian oscillations in both saline- and cocaine-treated WT mice followed similar patterns, indicating that the robustness of the oscillations is unchanged by cocaine (*SI Appendix*, Fig. S3*A*). Intriguingly, in WT livers, cocaine administration led to four times less oscillating acylcarnitines (Fig. 3*C*).

Twenty-five percent of circadian metabolites in iMSN-D2RKO livers lost rhythmicity after cocaine administration compared to saline-treated control mouse tissue (Fig. 3*D*). Conversely, 75% of oscillating metabolites in saline-treated iMSN-D2RKO mice were unaffected by cocaine administration.

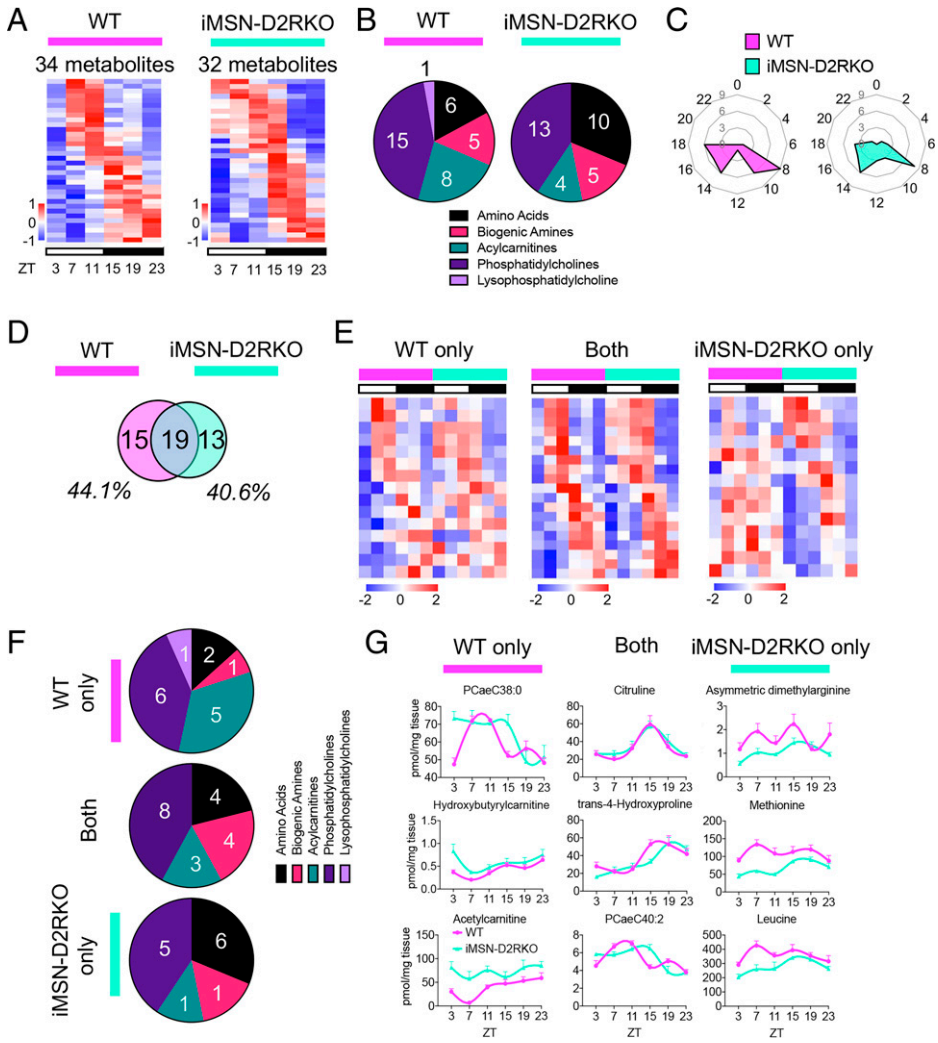

Fig. 2. Profiling of the circadian metabolome in iMSN-D2RKO mouse liver. (*A*) Heat maps of circadian metabolites in WT (*Left*, pink) or iMSN-D2RKO mouse liver (*Right*, blue). White and black bars indicate the light (ZT3, 7, and 11) and dark (ZT15, 19, and 23) time points, respectively. (*B*) Pie charts representing the percentage of metabolites of each class displaying rhythmic oscillations in WT (*Left*, pink) or iMSN-D2RKO mouse liver (*Right*, blue). (*C*) Radar plots displaying the phase analysis of metabolites cycling in WT (*Left*, pink) or iMSN-D2RKO mouse liver (*Right*, blue). (*D*) Venn diagram representing the hepatic rhythmic metabolites in WT (pink) and iMSN-D2RKO (blue) mice. (*E*) Heat maps of circadian metabolites exclusively in WT (pink) or iMSN-D2RKO mouse liver (blue) and commonly circadian in both (*Middle*). White and black bars indicate the light (ZT3, 7, and 11) and dark (ZT15, 19, and 23) time points, respectively. (*F*) Pie charts representing the percentage of metabolites of each class displaying rhythmic oscillations exclusively in WT (pink) or iMSN-D2RKO mouse liver (blue) and circadian in both genotypes (*Middle*). (*G*) Representative circadian profiles of metabolites oscillating in WT (pink) or iMSN-D2RKO mouse liver (blue) and circadian in both genotypes (*Middle*); $n = 5$, JTK_CYCLE, cutoff $P < 0.05$. All tissues used for analyses were collected from male mice.

Nevertheless, a staggering number of de novo oscillating metabolites were induced in iMSN-D2RKO livers after cocaine treatment compared to livers from saline-treated mice (Fig. 3 *D* and *E*). Treatments (saline or cocaine) did not affect the amplitude of the oscillations in iMSN-D2RKO liver metabolites (*SI Appendix*, Fig. S3*B*). Interestingly, the number of rhythmic acylcarnitines and phosphatidylcholines identified in the cocaine-treated iMSN-D2RKO mice increased well above that of saline-treated mice (Fig. 3*F*). Thus, loss of D2R signaling in the striatal iMSNs critically affects hepatic metabolism not only under basal conditions but also in response to a cocaine challenge.

Cocaine disrupts circadian gene expression and metabolic profiles in the striatum involving D2R-mediated regulation of iMSNs (22, 34). Thus, we analyzed and compared the full circadian metabolic profiles of livers from iMSN-D2RKO and WT mice given a single injection of cocaine at ZT3 (Fig. 3 *G*–*I*). No major changes were observed in the amplitude of oscillating metabolites common between cocaine-treated iMSN-D2RKO and WT mice (*SI Appendix*, Fig. S3*C*). Moreover, 16% of detected metabolites were oscillating in WT mice treated with cocaine, whereas up to ∼41% were oscillating in iMSN-D2RKO mice (Fig. 3*G*). Additionally, the phase of the identified circadian metabolites did not coincide between cocaine-treated WT and iMSN-D2RKO mice. In WT mice, the peak in rhythmicity during the light phase was observed around ZT8, whereas in iMSN-D2RKO mice, it shifted between ZT2 and ZT6. This difference in peak between the WT and iMSN-D2RKO cocaine-treated groups is not dependent on the injection itself, as all groups received an injection of saline or cocaine at the same time point. On the contrary, the dark-phase metabolite peak at about ZT16 remained consistent in both genotypes (Fig. 3*H*). Notably, in WT cocaine-treated mice, acylcarnitines comprised only ∼7% of oscillating metabolites in the liver but made up ∼30% of circadian metabolites in iMSN-D2RKO mice (Fig. 3*I*). Our data point to a striatal D2R-mediated control of circadian liver metabolites and show that dopamine signaling in the brain contributes to the regulation of liver physiology.

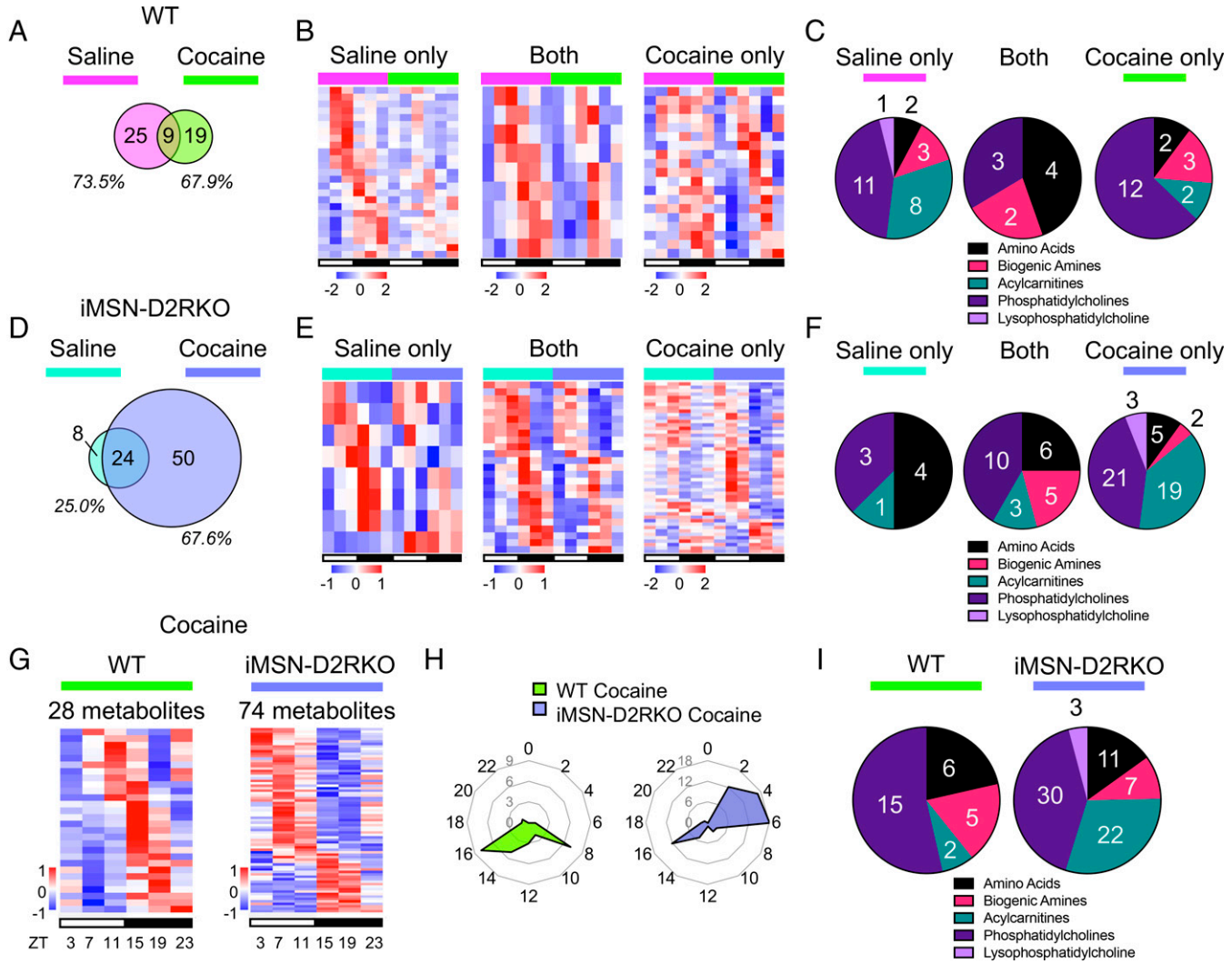

Fig. 3. Cocaine-induced disruption of liver circadian metabolites. (*A*) Venn diagram representing the hepatic rhythmic metabolites in saline-treated (pink) and cocaine-treated (green) WT mouse liver. (*B*) Heat maps of circadian metabolites exclusively in saline-treated (pink) or cocaine-treated (green) WT mouse liver and circadian in both (*Middle*). White and black bars indicate the light (ZT3, 7, and 11) and dark (ZT15, 19, and 23) time points, respectively. (*C*) Pie charts representing the percentage of metabolites of each class displaying rhythmic oscillations exclusively in saline-treated (pink) or cocaine-treated (green) WT mouse liver and circadian in both (*Middle*). (*D*) Venn diagram representing the hepatic rhythmic metabolites in saline-treated (blue) and cocaine-treated (purple) iMSN-D2RKO mouse liver. (*E*) Heat maps of circadian metabolites exclusively in saline-treated (blue) or cocaine-treated (purple) iMSN-D2RKO mouse liver and circadian in both (*Middle*). White and black bars indicate the light (ZT3, 7, and 11) and dark (ZT15, 19, and 23) time points, respectively. (*F*) Pie charts representing the percentage of metabolites of each class displaying rhythmic oscillations exclusively in saline-treated (blue) or cocaine-treated (purple) iMSN-D2RKO mouse liver and circadian in both (*Middle*). (*G*) Heat maps of circadian metabolites in livers of cocaine-treated WT (green) or iMSN-D2RKO mice (purple). White and black bars indicate the light (ZT3, 7, and 11) and dark (ZT15, 19, and 23) time points, respectively. (*H*) Radar plots displaying the phase analysis of metabolites cycling in livers of cocaine-treated WT (green) or iMSN-D2RKO mice (purple). (*I*) Pie charts representing the percentage of metabolites of each class displaying rhythmic oscillations in livers of cocaine-treated WT (green) or iMSN-D2RKO mice (purple); $n = 5$, JTK_CYCLE, cutoff $P < 0.05$. All tissues used for analyses were collected from male mice.

Effects of Cocaine on the Diurnal Liver Metabolome. Environmental cues, including light, food intake, and exercise, help maintain circadian synchrony of central and peripheral tissues (35). Disturbances to these cues can result in systemic clock desynchrony and have detrimental effects on organismal homeostasis (36). To determine time-of-day–dependent differences in metabolite levels in the liver, we compared the metabolomic profiles of cocaine-treated WT and iMSN-D2RKO mice during the light and dark phases at ZT11 and ZT23, the last time points in each phase, respectively (Fig. 4*A*). The majority of the metabolomic changes observed in the WT saline-treated mouse liver between ZT11 and ZT23 were found in phosphatidylcholines, acylcarnitines, and, to a lesser extent, biogenic amines ($P < 0.05$, ANOVA Benjamini–Hochberg corrected). Only after cocaine treatment did time-of-day–dependent metabolites in the WT liver include sphingomyelins and lysophosphatidylcholines ($P < 0.05$, ANOVA Benjamini–Hochberg corrected) (Fig. 4*A*). iMSN-D2RKO mice treated with cocaine show a striking decrease in the number of phosphatidylcholines that change with time in the liver ($P < 0.05$, ANOVA Benjamini–Hochberg corrected), an indication that a combination of cocaine and a loss of D2R greatly perturb phospholipid metabolism. A principal component analysis was performed to assess the correlation between and within the four experimental conditions: WT saline, WT cocaine, iMSN-D2RKO saline, and iMSN-D2RKO cocaine at each time point (*SI Appendix*, Fig. S4). When both time points were combined, no obvious correlation was determined among the four datasets, suggesting that the genotype × treatment interaction is influenced by time. Indeed, when separated by time point, clusters for each group were apparent, although less so at ZT23 (*SI Appendix*, Fig. S4). Further, we compared the up-regulation of

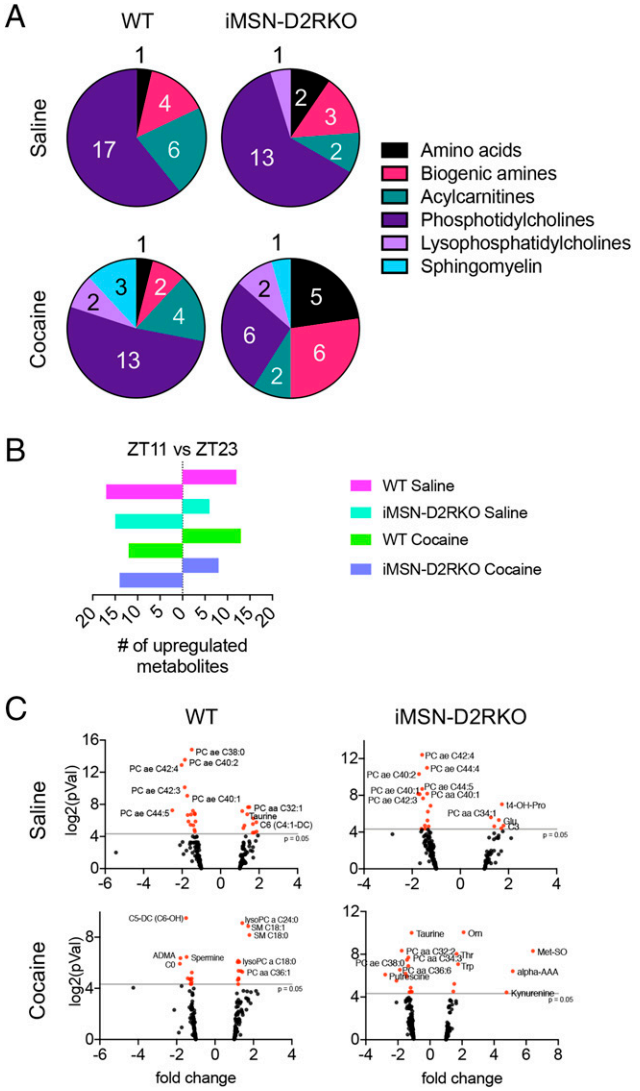

Fig. 4. Differential effects of cocaine on the liver metabolome. (*A*) Pie charts representing the percentage of liver metabolites of each class displaying different levels at ZT11 versus ZT23 in saline- or cocaine-treated WT or iMSN-D2RKO mice as indicated. (*B*) Number of metabolites up-regulated at either ZT11 or ZT23 in saline- or cocaine-treated mice as indicated. (*C*) Volcano plots of metabolites at ZT11 and ZT23 in livers from WT or iMSN-D2RKO mice treated with saline or cocaine. Metabolites with significant changes between time points were identified when the *P* value was <0.05 (red dots); $n = 5$, ANOVA Benjamini–Hochberg corrected, cutoff, $P < 0.05$; pVal, *P* value.

the metabolites at ZT11 and ZT23 (Fig. 4*B*). In the liver of saline-treated mice, we found that over 50% of the metabolites that change between time points exhibited higher levels during the dark phase (ZT23; $P < 0.05$, ANOVA Benjamini–Hochberg corrected). In the saline condition, a time-dependent up-regulation of phosphatidylcholines was observed at ZT23 in WT and iMSN-D2RKO livers (Fig. 4*C*). Surprisingly, cocaine reversed this trend and induced higher metabolite levels at ZT11 than at ZT23 in the livers of WT mice ($P < 0.05$, ANOVA Benjamini–Hochberg corrected) (Fig. 4*B*). Cocaine up-regulated lysophosphatidylcholines, sphingomyelins, and phosphatidylcholines in WT mice at ZT11 ($P < 0.05$, ANOVA Benjamini–Hochberg corrected). Conversely, at ZT11, livers of cocaine-treated iMSN-D2RKO mice showed an up-regulation primarily of amino acids and biogenic amines ($P < 0.05$, ANOVA Benjamini–Hochberg corrected). Taken together, our findings demonstrate that disrupted D2R signaling in iMSNs and an acute cocaine challenge alters temporal liver metabolism.

Discussion

Drugs of abuse hijack brain circuits that belong to the reward system. Indeed, all abused drugs elevate dopamine levels in the brain and most notably in the mesolimbic dopamine system, thereby generating pleasure and reward. The mesolimbic circuitry consists of dopaminergic projections arising from the midbrain and projecting to the striatum. The dorsal striatum is involved in decision-making, including initiation and action selection, controls habitual behavior, and mediates valiance and magnitude (4–6). Relatedly, the ventral striatum, in particular the NAcc, is most appreciated for its involvement in reward processing and evaluation as well as incentive-based learning (7–9). The connections and mechanisms linking different neurons to the generation of reward is a topic of great importance and interest (37, 38). The major constituents of the striatum, the MSNs, serve as this brain structure's exclusive output neurons (39). Human studies have shown that people with addiction have decreased D2R binding availability in the striatum regardless of the class of drug being used (40). Thus, our iMSN-D2RKO mouse appears to be a good candidate to model this human condition, as this model has a deletion of D2R throughout the dorsal and ventral regions of the striatum. Despite the presence of cocaine, loss of D2R results in reduced movement and locomotor behavior (Fig. 1*B*) (26). The absence of D2R alone alters a number of metabolic parameters, including body weight, food intake, energy expenditure, and fat tissue accumulation (Fig. 1 *C*–*E*). As expected, these metabolic parameters changed in a time-of-day–dependent manner due to the intimate link between metabolism and the circadian clock. Thus, to further investigate the contributions of D2R on metabolism, we performed metabolomic analysis on the livers of WT and iMSN-D2RKO littermates throughout a full circadian cycle for a greater time point resolution.

The cell-specific loss of D2R did not change the overall circadian parameters of the metabolites in the liver (Fig. 2). Yet, quite surprisingly, we demonstrate that the changes induced in the absence of D2R are found in the distribution of the number of oscillating metabolites of each class. Notably, acylcarnitines show the greatest change to the number of oscillating metabolites that lose rhythmicity in the iMSN-D2RKO mouse liver and instead display constitutively higher levels throughout the day. Of these, we have identified hydroxybutyrylcarnitine as a metabolite significantly rhythmic in WT but not in iMSN-D2RKO mice. Previous studies demonstrate a strong association between acylcarnitines and insulin resistance in people suffering from type 2 diabetes (41, 42).

The peripheral metabolic impact of the loss of striatal D2R signaling could be clearly seen in the presence of cocaine. Indeed, this dopaminergic challenge resulted in almost threefold more oscillating metabolites in cocaine-treated iMSN-D2RKO mice than in WT controls (Fig. 3*A*). A large number of these metabolites could be the result of an increase in metabolites oscillating between ZT2 and ZT6 in iMSN-D2RKO mice that is not present in WT mice (Fig. 3*B*). Importantly, we found that acylcarnitines and phosphatidylcholines were metabolite classes in the liver highly altered by cocaine administration in iMSN-D2RKO. It can be argued that some of the observed changes can be ascribed to genetic manipulation of the D2R gene or to the CRE line used to obtain iMSN-D2RKO mice. While we cannot completely exclude this possibility, we are confident that this is not the case. In support of our findings, changes of these metabolites were also found by NMR in the blood of crack-cocaine addicts (43).

The liver uses excess glucose from food and converts it into fatty acids, which are stored as visceral fat to promote

long-term energy storage. We find that the iMSN-D2RKO animals have a higher fat-to-body weight ratio than WT littermates (Fig. 1*F*). Lipidomic analyses of cocaine-treated mice discovered that an increase in lipid metabolism resulted in a protective effect against hepatotoxicity (31). The changes we observed in the lipid metabolites may be attributed to an additive accumulation of liver insults induced by cocaine and indirectly by the loss of D2R. Communication between the suprachiasmatic nucleus and the striatum have been recently identified (44, 45). The neurochemistry of these connections may be affected in the absence of D2R in iMSNs, which could then result in a dysregulation of peripheral organs, including the liver. Recent work has shown that the nuclear receptor PPARγ plays a role in inducing changes to the molecular clock in the striatum in an iMSN-D2R–dependent manner (22). We might speculate that through striatal D2R signaling, cocaine might induce a proinflammatory response that affects liver function.

A high-fat dietary challenge proved to have substantial effects on circadian metabolite coordination between tissues (27). Metabolic intertissue communication is highly dynamic and easily influenced by external factors introduced to the body. Our findings support this notion, as cocaine, a dopaminergic challenge, has a striatal-dependent impact on the liver, with a more striking effect in the absence of D2R in iMSNs (Fig. 4). Here, using light- and dark-phase time points (ZT11 and ZT23, respectively), we identified liver metabolites changing in a time-dependent manner. Intriguingly, cocaine induced altered levels of sphingomyelins in the liver. Sphingomyelins, typically associated with neuronal axons, when detected in the liver can serve as biomarkers for hepatotoxicity and liver damage (46, 47). Future studies will be aimed at examining the specific metabolites identified in greater detail to unravel the mechanisms underlying the regulation of liver rhythmicity by striatal D2R signaling. Our results lead us to conclude that challenging the dopaminergic reward system by cocaine use and altered striatal D2R signaling can contribute to the progression of metabolic diseases.

In this study, we take an unconventional angle to study the effects of the dopaminergic pathways and the consequences of drugs of abuse on the periphery. We identify that the circadian metabolic state of the liver in iMSN-D2RKO mice is more prone to induce de novo rhythmic acylcarnitines after a cocaine challenge. Importantly, our findings also show that the desynchrony between the liver and striatum, in the absence of D2R in a neuron-type–specific manner, influences liver homeostasis, only to be heightened by cocaine. These findings link metabolites to drug use–mediated alterations in the brain affecting peripheral tissues. Based on our data, it is tempting to propose a tight association between drug use and the increased susceptibility to metabolic diseases (48–53) via altered modulation of acylcarnitines and sphingomyelins in the liver. Future studies should seek to identify other key players of the intertissue communication in an effort to prevent drug use–induced metabolic disorders.

Methods

Animals. Three-month-old male iMSN-D2RKO mice were generated by mating $D2R^{flox/flox}$ mice (WT) with $D2R^{flox/flox/D1R\text{-}CRE+/-}$ mice (iMSN-D2RKO) with a genetic background of 98.44% C57BL6 × 1.56% 129SV mouse strains (54). The ability of D1R CRE to eliminate D2R in iMSNs stems from the common expression of D1R and D2R in embryonic MSN precursors (55). D2R ablation in iMSNs was previously confirmed by recording D2R-specific binding using ^{3}H-labeled ligand on striatal extracts as well as in situ hybridization experiments using riboprobes targeting GAT1 as an MSN marker and exon 2 of D2R (54). Mice were maintained on a standard 12-h light/12-h dark cycle; food and water were available ad libitum in ∼25 °C; humidity was 40 to 60%. Animal care and use was in accordance with guidelines of the Institutional Animal Care and Use Committee at the University of California, Irvine. Genotype identification was performed by Southern blot and PCR analyses of DNA extracted from tail biopsies.

Motor Activity and Food Intake. Motor activity was measured using actimetric boxes with a photo beam system and recorded with Lab watcher software. WT and iMSN-D2RKO mice were single housed during testing. Beam breaks (counts)/minute were averaged every 12 h during the light cycle (6:30 AM to 6:30 PM) and during the dark cycle (6:30 PM to 6:30 AM) or every hour. Chow intake was measured every day for 5 consecutive days at 6:00 PM. Food intake was calculated as the grams of food consumed in 24 h over the body weight of the mouse.

RNA Extraction, Reverse Transcription, and Quantitative Real-Time Polymerase Chain Reaction Analyses. Total RNA was extracted from mouse liver tissue using TRIzol (Invitrogen, catalog no. 15596026) following manufacturer's recommendation. Total RNA (1 μg) was reverse-transcribed to synthesize cDNA using Maxima H Minus cDNA Synthesis Master Mix (ThermoFisher Scientific, catalog no. M1662), according to manufacturer's protocol. cDNA (1:10) was used for quantitative real-time PCR using PowerUp SYBR Master Mix (ThermoFisher Scientific, catalog no. A25741) and ran on a QuantStudio 3 Real-Time PCR System. Gene expression was normalized to 18S rRNA (1:500 cDNA). Primer sequences used for gene expression analyses were as follows: m*Dbp* Fwd: 5′-AATGACCTTTGAACCTGATCCCGCT-3′, Rev: 5′- GCTCCAGTACTTCTCATCCTTCTGT-3′. m*Bmal1* Fwd: 5′-GCAGTGCCACTGACTACCAAGA-3′, Rev: 5′- TCCTGGACATTGCATTGCAT-3′. m*Per1* Fwd: 5′-ACCAGCGTGTCATGATGACATA-3′, Rev: 5′- GTGCACAGCACCCAGTTCCC-3′. m*Cpt1a* Fwd: 5′-TGACTGGTGGGAGGAATACA-3′, Rev: 5′- AGTATGG CGTGGATGGTGTT-3′. The 18S rRNA Fwd: 5′-CGCCGCTAGAGGTGAAATTC-3′, Rev: 5′-CGAACCTCCGACTTTCGTTCT-3′.

Cocaine Treatment. Before cocaine treatments, mice were handled for at least 3 d for 5 min. On the day of treatment, mice were administered either cocaine or saline. Cocaine (Sigma, catalog no. C5776) was dissolved in saline (NaCl 0.9%) and injected intraperitoneally at a dose of 20 mg kg^{-1}.

Metabolomics Analyses. Metabolite levels were measured from WT and iMSN-D2RKO mouse liver tissue harvested at ZT3, 7, 11, 15, 19 and 23 after an intraperitoneal injection of saline or cocaine at a dose of 20 mg kg^{-1} at ZT3; five replicates were used/time point/treatment. Metabolomic analyses were performed by Biocrates focusing on metabolites critical for neuronal structure, function, and signaling (56, 57) using the AbsoluteIDQ p180 platform. Briefly, to extract metabolites from liver tissue, the samples were first suspended in an 85% ethanol/15% 10 mM phosphate buffer (pH 7.4), using 3 μL of extraction buffer per milligram of wet weight. The samples were then sonicated, vortexed, and homogenized using a Precellys-24 instrument (Bertin Technologies). After homogenization, an aliquot of each supernatant was centrifuged and used for metabolomics measurements.

The measurements were run according to the AbsoluteIDQ p180 kit manufacturer's instructions. The experimental metabolomics measurement technique is described in detail by patents EP1897014B1 (https://patents.google.com/patent/EP1897014B1) and EP1875401B1 (https://patents.google.com/patent/EP1875401B1). In short, Biocrates' commercially available kit plates were used for the quantification of amino acids, acylcarnitines, sphingomyelins, phosphatidylcholines, hexoses, and biogenic amines. The fully automated assay was based on phenyl isothiocyanate derivatization in the presence of internal standards, followed by flow injection analysis-tandem mass spectrometry for acylcarnitines, lipids, and hexose and liquid chromatography-tandem mass spectrometry for amino acids and biogenic amines using an AB SCIEX 4000 QTrap mass spectrometer (AB SCIEX) with electrospray ionization. Data were quantified using Sciex Analyst and imported into the Biocrates MetIDQ software for further analysis.

Statistics and Bioinformatics Analyses. Statistical and bioinformatics analyses were performed based on pairwise comparisons, where the effect of cocaine treatment was analyzed while controlling the genotype or the difference between genotypes (WT or iMSN-D2RKO) were compared while controlling the treatment. Dixon's test was performed to reduce outlier effects, filtering out up

to one outlier replicate from each condition. Heat maps for the metabolite profiles were generated using the RStudio software. Row *z* scores are displayed and were calculated using the "heatmap.2" function of the gplots package. GraphPad Prism 9.2.0 was used to perform statistical analyses and generate principal component analysis plots. Two-way ANOVA or a two-way ANOVA mixed-effects model followed by Tukey's multiple comparison post hoc test was used as appropriate; a P value of <0.05 was considered statistically significant. Values are presented as mean ± SEM. ANOVA Benjamini–Hochberg-corrected statistical analysis was performed to calculate the time-dependent effects.

Data Availability. All metabolomic data are included in the article and/or supporting information.

ACKNOWLEDGMENTS. We thank all the members of the E.B. and P.S.-C. laboratories for scientific discussion. We appreciate K. Brami-Cherrier and D. Radl for their initial interest in this work. M.C. was supported by predoctoral fellowships from the NIH (F31GM117942) and the American Heart Association (17PRE33410952). R.G.L. was supported by a University of California, Irvine School of Medicine Dean's Fellowship, the Dr. Lorna Carlin Scholar Award, a University of California, Irvine Graduate Dean's Dissertation Fellowship, and a National Institute on Drug Abuse T32 Predoctoral Training Grant (DA050558-02). M.A.D.-F. was a recipient of FP7 Marie Curie Actions grant agreement COFUND N.267232 Project I-MOVE n.13001106001802512447. This work was supported by grants from the NIH (DA035600 to E.B. and P.S.-C.) and by the French Institut National de la Santé et de la Recherche Médicale (INSERM).

1. B. F. Grant *et al.*, Epidemiology of DSM-5 drug use disorder: Results from the national epidemiologic survey on alcohol and related conditions-III. *JAMA Psychiatry* **73**, 39–47 (2016).
2. G. Di Chiara, A. Imperato, Drugs abused by humans preferentially increase synaptic dopamine concentrations in the mesolimbic system of freely moving rats. *Proc. Natl. Acad. Sci. U.S.A.* **85**, 5274–5278 (1988).
3. E. J. Nestler, Cellular basis of memory for addiction. *Dialogues Clin. Neurosci.* **15**, 431–443 (2013).
4. B. W. Balleine, M. R. Delgado, O. Hikosaka, The role of the dorsal striatum in reward and decision-making. *J. Neurosci.* **27**, 8161–8165 (2007).
5. A. C. Burton, K. Nakamura, M. R. Roesch, From ventral-medial to dorsal-lateral striatum: Neural correlates of reward-guided decision-making. *Neurobiol. Learn. Mem.* **117**, 51–59 (2015).
6. D. M. Lipton, B. J. Gonzales, A. Citri, Dorsal striatal circuits for habits, compulsions and addictions. *Front. Syst. Neurosci.* **13**, 28 (2019).
7. A. Alcaro, R. Huber, J. Panksepp, Behavioral functions of the mesolimbic dopaminergic system: An affective neuroethological perspective. *Brain Res. Brain Res. Rev.* **56**, 283–321 (2007).
8. W. Schultz, P. Apicella, E. Scarnati, T. Ljungberg, Neuronal activity in monkey ventral striatum related to the expectation of reward. *J. Neurosci.* **12**, 4595–4610 (1992).
9. R. Daniel, S. Pollmann, A universal role of the ventral striatum in reward-based learning: Evidence from human studies. *Neurobiol. Learn. Mem.* **114**, 90–100 (2014).
10. G. A. Graveland, M. DiFiglia, The frequency and distribution of medium-sized neurons with indented nuclei in the primate and rodent neostriatum. *Brain Res.* **327**, 307–311 (1985).
11. M. K. Lobo, E. J. Nestler, The striatal balancing act in drug addiction: Distinct roles of direct and indirect pathway medium spiny neurons. *Front. Neuroanat.* **5**, 41 (2011).
12. R. W. Logan, W. P. Williams III, C. A. McClung, Circadian rhythms and addiction: Mechanistic insights and future directions. *Behav. Neurosci.* **128**, 387–412 (2014).
13. B. P. Hasler, L. J. Smith, J. C. Cousins, R. R. Bootzin, Circadian rhythms, sleep, and substance abuse. *Sleep Med. Rev.* **16**, 67–81 (2012).
14. G. Asher, P. Sassone-Corsi, Time for food: The intimate interplay between nutrition, metabolism, and the circadian clock. *Cell* **161**, 84–92 (2015).
15. C. B. Green, J. S. Takahashi, J. Bass, The meter of metabolism. *Cell* **134**, 728–742 (2008).
16. C. L. Partch, C. B. Green, J. S. Takahashi, Molecular architecture of the mammalian circadian clock. *Trends Cell Biol.* **24**, 90–99 (2014).
17. J. Bass, M. A. Lazar, Circadian time signatures of fitness and disease. *Science* **354**, 994–999 (2016).
18. D. K. Welsh, J. S. Takahashi, S. A. Kay, Suprachiasmatic nucleus: Cell autonomy and network properties. *Annu. Rev. Physiol.* **72**, 551–577 (2010).
19. U. Albrecht, Timing to perfection: The biology of central and peripheral circadian clocks. *Neuron* **74**, 246–260 (2012).
20. J. A. Mohawk, C. B. Green, J. S. Takahashi, Central and peripheral circadian clocks in mammals. *Annu. Rev. Neurosci.* **35**, 445–462 (2012).
21. K. L. Eckel-Mahan *et al.*, Reprogramming of the circadian clock by nutritional challenge. *Cell* **155**, 1464–1478 (2013).
22. K. Brami-Cherrier *et al.*, Cocaine-mediated circadian reprogramming in the striatum through dopamine D2R and PPARγ activation. *Nat. Commun.* **11**, 4448 (2020).
23. N. D. Volkow, G.-J. Wang, R. D. Baler, Reward, dopamine and the control of food intake: Implications for obesity. *Trends Cogn. Sci.* **15**, 37–46 (2011).
24. J. D. Salamone, Complex motor and sensorimotor functions of striatal and accumbens dopamine: Involvement in instrumental behavior processes. *Psychopharmacology (Berl.)* **107**, 160–174 (1992).
25. K. E. Foster-Schubert *et al.*, Effect of diet and exercise, alone or combined, on weight and body composition in overweight-to-obese postmenopausal women. *Obesity (Silver Spring)* **20**, 1628–1638 (2012).
26. G. Kharkwal, D. Radl, R. Lewis, E. Borrelli, Dopamine D2 receptors in striatal output neurons enable the psychomotor effects of cocaine. *Proc. Natl. Acad. Sci. U.S.A.* **113**, 11609–11614 (2016).
27. K. A. Dyar *et al.*, Atlas of circadian metabolism reveals system-wide coordination and communication between clocks. *Cell* **174**, 1571–1585 (2018).
28. K. L. Eckel-Mahan *et al.*, Coordination of the transcriptome and metabolome by the circadian clock. *Proc. Natl. Acad. Sci. U.S.A.* **109**, 5541–5546 (2012).
29. S. Masri *et al.*, Partitioning circadian transcription by SIRT6 leads to segregated control of cellular metabolism. *Cell* **158**, 659–672 (2014).
30. Y. Adamovich *et al.*, Circadian clocks and feeding time regulate the oscillations and levels of hepatic triglycerides. *Cell Metab.* **19**, 319–330 (2014).
31. R. Aviram *et al.*, Lipidomics analyses reveal temporal and spatial lipid organization and uncover daily oscillations in intracellular organelles. *Mol. Cell* **62**, 636–648 (2016).
32. S. Y. Krishnaiah *et al.*, Clock regulation of metabolites reveals coupling between transcription and metabolism. *Cell Metab.* **25**, 961–974 (2017).
33. M. E. Hughes, J. B. Hogenesch, K. Kornacker, JTK_CYCLE: An efficient nonparametric algorithm for detecting rhythmic components in genome-scale data sets. *J. Biol. Rhythms* **25**, 372–380 (2010).
34. W. J. Lynch, M. J. Girgenti, F. J. Breslin, S. S. Newton, J. R. Taylor, Gene profiling the response to repeated cocaine self-administration in dorsal striatum: A focus on circadian genes. *Brain Res.* **1213**, 166–177 (2008).
35. Y. Tahara, S. Aoyama, S. Shibata, The mammalian circadian clock and its entrainment by stress and exercise. *J. Physiol. Sci.* **67**, 1–10 (2017).
36. A. Patke, M. W. Young, S. Axelrod, Molecular mechanisms and physiological importance of circadian rhythms. *Nat. Rev. Mol. Cell Biol.* **21**, 67–84 (2020).
37. B. Knutson, C. M. Adams, G. W. Fong, D. Hommer, Anticipation of increasing monetary reward selectively recruits nucleus accumbens. *J. Neurosci.* **21**, RC159 (2001).
38. S. Ikemoto, J. Panksepp, The role of nucleus accumbens dopamine in motivated behavior: A unifying interpretation with special reference to reward-seeking. *Brain Res. Brain Res. Rev.* **31**, 6–41 (1999).
39. J.-A. Girault, "Integrating neurotransmission in striatal medium spiny neurons" in *Synaptic Plasticity: Dynamics, Development and Disease*, M. R. Kreutz, C. Sala, Eds. (Advances in Experimental Medicine and Biology, Springer, 2012), pp. 407–429.
40. N. D. Volkow *et al.*, Decreased striatal dopaminergic responsiveness in detoxified cocaine-dependent subjects. *Nature* **386**, 830–833 (1997).
41. M. R. Soeters, P. B. Soeters, M. G. Schooneman, S. M. Houten, J. A. Romijn, Adaptive reciprocity of lipid and glucose metabolism in human short-term starvation. *Am. J. Physiol. Endocrinol. Metab.* **303**, E1397–E1407 (2012).
42. M. G. Schooneman, F. M. Vaz, S. M. Houten, M. R. Soeters, Acylcarnitines: Reflecting or inflicting insulin resistance? *Diabetes* **62**, 1–8 (2013).
43. T. B. B. C. Costa *et al.*, Insights into the effects of crack abuse on the human metabolome using a NMR approach. *J. Proteome Res.* **18**, 341–348 (2019).
44. S. Miyazaki *et al.*, Chronic methamphetamine uncovers a circadian rhythm in multiple-unit neural activity in the dorsal striatum which is independent of the suprachiasmatic nucleus. *Neurobiol. Sleep Circadian Rhythms* **11**, 100070 (2021).
45. M. Verwey, S. Dhir, S. Amir, Circadian influences on dopamine circuits of the brain: Regulation of striatal rhythms of clock gene expression and implications for psychopathology and disease. *F1000Res* **5**, F1000 (2016).
46. J. Simon *et al.*, Sphingolipids in non-alcoholic fatty liver disease and hepatocellular carcinoma: Ceramide turnover. *Int. J. Mol. Sci.* **21**, 40 (2019).
47. M. Apostolopoulou *et al.*, Specific hepatic sphingolipids relate to insulin resistance, oxidative stress, and inflammation in nonalcoholic steatohepatitis. *Diabetes Care* **41**, 1235–1243 (2018).
48. E. A. Warner, G. S. Greene, M. S. Buchsbaum, D. S. Cooper, B. E. Robinson, Diabetic ketoacidosis associated with cocaine use. *Arch. Intern. Med.* **158**, 1799–1802 (1998).
49. T. R. Drake, T. Henry, J. Marx, P. A. Gabow, Severe acid-base abnormalities associated with cocaine abuse. *J. Emerg. Med.* **8**, 331–334 (1990).
50. A. Virmani, Z. K. Binienda, S. F. Ali, F. Gaetani, Metabolic syndrome in drug abuse. *Ann. N. Y. Acad. Sci.* **1122**, 50–68 (2007).
51. J. A. Henry, Metabolic consequences of drug misuse. *Br. J. Anaesth.* **85**, 136–142 (2000).
52. M. A. Della Fazia, G. Servillo, Foie gras and liver regeneration: A fat dilemma. *Cell Stress* **2**, 162–175 (2018).
53. N. Li, H. Zhao, Role of carnitine in non-alcoholic fatty liver disease and other related diseases: An update. *Front. Med. (Lausanne)* **8**, 689042 (2021).
54. A. Anzalone *et al.*, Dual control of dopamine synthesis and release by presynaptic and postsynaptic dopamine D2 receptors. *J. Neurosci.* **32**, 9023–9034 (2012).
55. O. Aizman *et al.*, Anatomical and physiological evidence for D1 and D2 dopamine receptor colocalization in neostriatal neurons. *Nat. Neurosci.* **3**, 226–230 (2000).
56. R. M. Adibhatla, J. F. Hatcher, Role of lipids in brain injury and diseases. *Future Lipidol.* **2**, 403–422 (2007).
57. D. Piomelli, G. Astarita, R. Rapaka, A neuroscientist's guide to lipidomics. *Nat. Rev. Neurosci.* **8**, 743–754 (2007).